

See discussions, stats, and author profiles for this publication at: <https://www.researchgate.net/publication/274258852>

# Early Stage P22 Viral Capsid Self-Assembly Mediated by Scaffolding Protein: Atom-Resolved Model and Molecular Dynamics Simulation

ARTICLE *in* THE JOURNAL OF PHYSICAL CHEMISTRY B · MARCH 2015

Impact Factor: 3.3 · DOI: 10.1021/acs.jpcb.5b00303 · Source: PubMed

---

READS

15

## 4 AUTHORS, INCLUDING:



[Yuriy Sereda](#)

Indiana University Bloomington

40 PUBLICATIONS 89 CITATIONS

[SEE PROFILE](#)

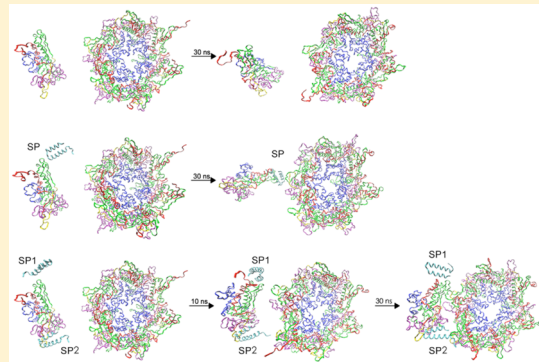
# Early Stage P22 Viral Capsid Self-Assembly Mediated by Scaffolding Protein: Atom-Resolved Model and Molecular Dynamics Simulation

Jiajian Jiang, Jing Yang, Yuriy V. Sereda, and Peter J. Ortoleva\*

Center for Theoretical and Computational Nanoscience, Department of Chemistry, Indiana University, Bloomington, Indiana 47405, United States

Supporting Information

**ABSTRACT:** Molecular dynamics simulation of an atom-resolved bacteriophage P22 capsid model is used to delineate the underlying mechanism of early stage P22 self-assembly. A dimer formed by the C-terminal fragment of scaffolding protein with a new conformation is demonstrated to catalyze capsomer (hexamer and pentamer) aggregation efficiently. Effects of scaffolding protein/coat protein binding patterns and scaffolding protein concentration on efficiency, fidelity, and capsid curvature of P22 self-assembly are identified.



## 1. INTRODUCTION

The mechanism of icosahedral bacteriophage self-assembly is of long-term and widespread interest, from the perspective of both clarifying the construction of complex capsid structure via assembly of small subunits,<sup>1,2</sup> as well as the potential applications to the fields of antiviral drug<sup>3</sup> and capsid-based nanoplatform design.<sup>4–7</sup> For simple viral capsids, a geometrical model was proposed to describe the self-assembly as aggregation of similar subunits into an icosahedral shell.<sup>8</sup> However, in self-assembly of more complex capsids (e.g., T4, lambda, P22), a scaffolding protein (SP) was demonstrated to be necessary. Particularly, during P22 viral capsid self-assembly, it was suggested that SPs copolymerize with capsid proteins, also known as coat proteins (CPs), and subsequently catalyze the aggregation of CPs.<sup>9,10</sup> Further studies revealed that the recognition and binding between SPs and CPs are mainly contributed by electrostatic interaction,<sup>11,12</sup> and the efficiency of P22 self-assembly is influenced by the SP/CP concentration ratio.<sup>13,14</sup> SPs were also observed to participate in both the nucleation and growth phases of self-assembly,<sup>14,15</sup> but leave reversibly during the procapsid-to-capsid structural transformation.<sup>16,17</sup>

The icosahedral structure formation of the capsid was generally described by a geometric principle which suggested that pentamers served as convex surfaces introducing particular curvature in the hexamers planar.<sup>18</sup> SP was also demonstrated to be critical for P22 capsid curvature regulation. In the absence of SPs,  $T = 4$  capsids form during self-assembly in addition to wild-type  $T = 7$  capsid. Several hypotheses were suggested to explain SP's roles. (1) CP/SP binding changes CP conformations, facilitating  $T = 7$  capsid formation. (2) CP/SP binding at the junction of capsomers influences capsomer placement. (3) Steric effect induced by SP regulates overall capsid curvature.<sup>19</sup>

The structure of P22 capsid (Figure 1a) implies that there are two conformations (intracapsomer and intercapsomer) of neighboring CP monomers. Kinetic analysis of the polymerization of SP and CP suggested that CP pentamers initially serve as nucleation seeds. However, P22 polymerization was suggested to be different from those of other capsids (picornaviruses, papovaviruses, HK97, etc.) and still remains elusive. The complexity of P22 self-assembly is possibly due to the requirements of packaging DNA and structural transformation during the capsid maturation.<sup>15,20</sup>

In addition to SP monomer, SP polymer was demonstrated to participate in P22 self-assembly.<sup>14,15,21</sup> In the mutation study, a covalently bonded SP dimer (R74C/L177I) was proven to catalyze self-assembly more efficiently compared with wild-type SP monomer.<sup>20,21</sup> SP dimer was indicated to be critical for the high fidelity of the formation of  $T = 7$  capsid as well.<sup>22</sup>

The complete structure of SP is not yet determined, while a C-terminal fragment of SP, also called CP-binding domain, was identified to exhibit a helix-loop-helix motif and be sufficient to catalyze capsid self-assembly (Figure 1b).<sup>12</sup> Deletion analysis showed that residues 280–294 were the minimum region required for SP to bind CP mainly through electrostatic interaction.<sup>23,24</sup> Also, with five structural domains of CP defined previously (Figure 1c),<sup>25</sup> part of the SP-binding sites were believed to be on the N-arm and the A-domain of CP.<sup>26–28</sup>

The abundant experimental results make P22 capsid an ideal system for computational analysis. Previous studies of capsid self-assembly were carried out using coarse-grained models of capsid

Received: January 11, 2015

Revised: March 25, 2015

Published: March 27, 2015

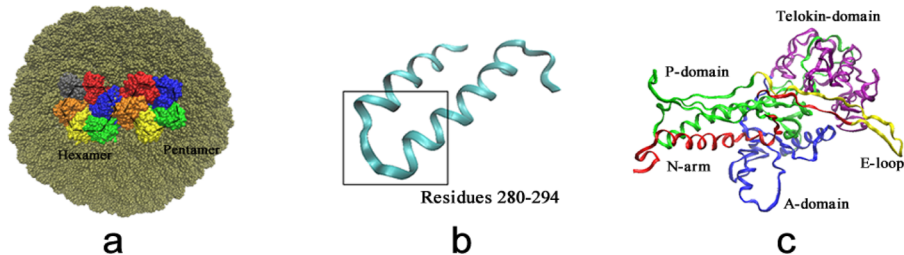


**Figure 1.** Atom-resolved models used in the molecular dynamics simulation. (a) P22 capsid (PDB ID: 2XYY), composed of 60 CP hexamers and 12 CP pentamers (around 2 millions atoms). (b) C-terminal fragment of SP, residues 280 to 294 were proposed to be the minimum CP-binding region (PDB ID: 1GP8). (c) CP monomer structure, 5 structural domains are labeled with different colors: red region is N-arm; green region is P-domain; purple region is Telokin-domain; yellow region is E-loop; blue region is A-domain.

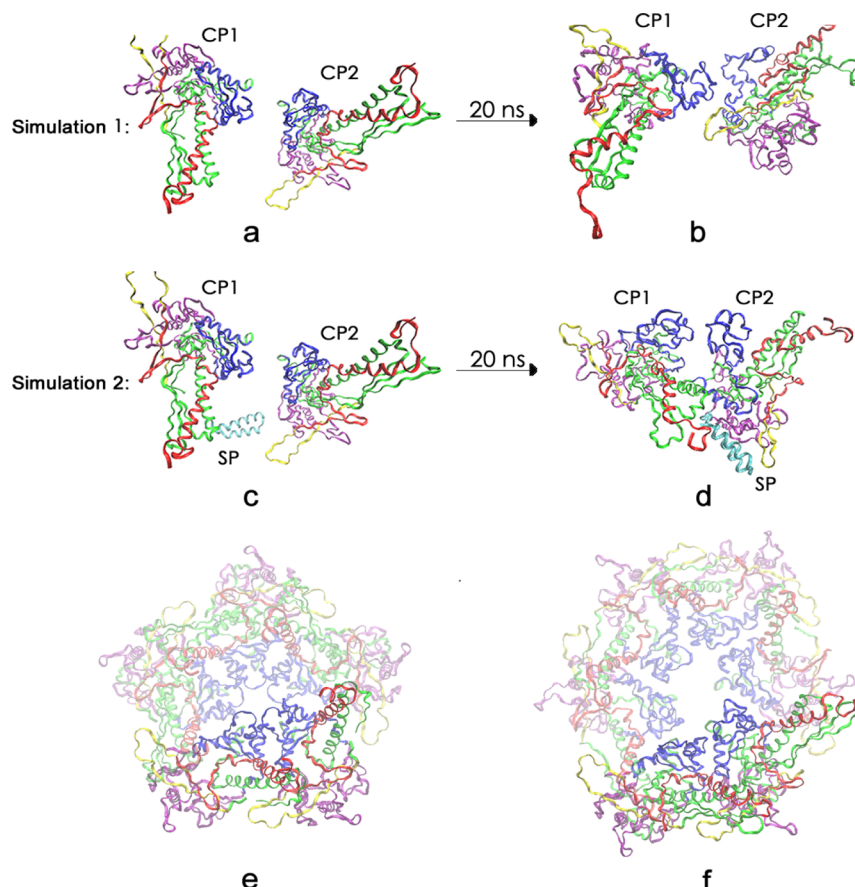


**Figure 2.** Simulations 1–2: intracapsomer dimerization of CP monomer for 20 ns. (a) SP C-terminal free initial configuration of CP monomers. (b) Configuration after 20 ns of simulation 1. (c) Initial configuration of CP monomers with a SP C-terminal near the N-arm/P-domain of one of the CP monomers. (d) Configuration after 20 ns of simulation 2. (e) CP pentamer, opaque region is the neighboring CP monomers. (f) CP hexamer, opaque region is the neighboring CP monomers. The main characteristics of (d) are similar to those of opaque region of (e) and (f): the attachments occur between the A-domains (blue), and the similar angles are achieved between the N-arms/P-domains (red/green) of CP monomers.

subunits.<sup>29–34</sup> While the self-assembly could be efficiently simulated, the subtle details missing in the coarse-graining and structure recalibration may limit the credibility of these modeling methods. Molecular dynamics (MD) is a powerful tool for simulating the behavior of biological systems by providing richness of dynamical details.<sup>30,35,36</sup> In this study, an atom-resolved P22 model is built (see Supporting Information) as the initial configuration used in MD to delineate the mechanism of P22 early stage self-assembly, and experimental results are used to evaluate the simulations. Initially, the SP C-terminal mediated intracapsomer dimerization of CP monomer is presented (section 2.1), with SP C-terminal/CP binding patterns obtained;

then SP C-terminal mediated intercapsomer complexing of CP monomer and capsomer is shown, with binding patterns of SP C-terminal and CP monomer/capsomer collected as well, and a discussion of SP concentration effect on the efficiency and fidelity of self-assembly (section 2.2). Finally, a SP C-terminal dimer with new conformation is proposed, and SP C-terminal mediated aggregation of CP capsomers is revealed, with capsid curvature formation discussed (section 2.3).

## 2. RESULTS AND DISCUSSION

### 2.1. SP C-Terminal Mediated Intracapsomer Dimerization of CP Monomer.

To explore the role of SP C-terminal in

**Table 1.** SP C-Terminal Binding Sites in CP Monomer Collected from Simulation 2

structural domains	binding residues in CP1	binding residues in CP2
N-arm	5–15	-
P-domain	90–100	-
A-domain	-	153
Telokin-domain	-	320–336

the intracapsomer dimerization of CP monomer, two 20 ns simulations are performed with the same configuration of two CP monomers (Figure 2a and c). In simulation 2, one SP C-terminal is added near the N-arm/P-domain of a CP monomer, which was proposed to contain part of the SP-binding sites.<sup>27</sup> The SP C-terminal free dimerization of CP monomer produces a configuration (Figure 2b) that does not match the neighboring CP monomers in a capsomer (Figure 2e,f). In contrast, a different pathway is shown with the addition of the SP C-

**Table 2.** SP C-Terminal Binding Sites in CP Monomer/Capsomer Collected from Simulations 4–5

simulation	structural domains	binding residues in CP	binding residues in hexamer
4	N-arm	10–12	-
5 (10 ns)	P-domain	394–401	-
	Telokin-domain	-	310–312
	N-arm	10	-
5 (30 ns)	P-domain	399	396–399
	E-loop	70–72	63–65
	N-arm	11–14	-
5 (30 ns)	P-domain	397–399	86–92, 398–400
	E-loop	66–71	63–67

terminal. The main characteristics of the configuration after 20 ns of simulation 2 (Figure 2d) are consistent with those of neighboring CP monomers in a capsomer. These simulation

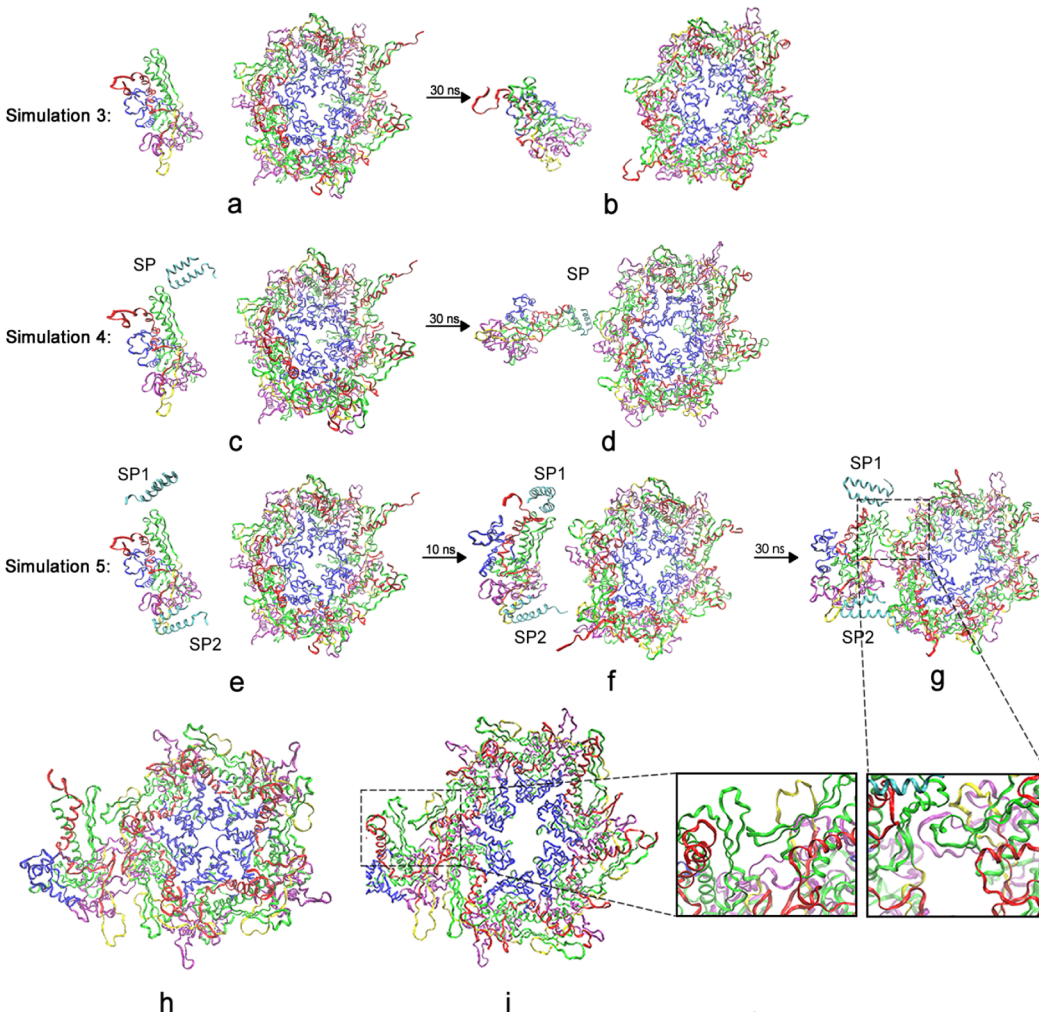


**Figure 3.** Simulations 3–5: SP C-terminal mediated intercapsomer complexing of CP monomer and hexamer. (a) SP C-terminal free initial configuration in simulation 3. (b) Configuration after 30 ns of simulation 3. (c) Initial configuration in simulation 4, with one SP C-terminal near the N-arm/P-domain of CP monomer. (d) Configuration after 30 ns of simulation 4, with the N-arm/P-domain of CP monomer approaching the hexamer. (e) Initial configuration in simulation 5, with two SP C-terminals near the N-arm/P-domain and E-loop of CP monomer. (f) Configuration after 10 ns of simulation 5, CP monomer approaches the hexamer. (g) Configuration after 30 ns of simulation 5, attachment of CP monomer and hexamer is observed. (h) Configuration of a pentamer plus a neighboring CP subunit. (i) Configuration of a hexamer plus a neighboring CP subunit. The structures (g) and (i) are similar: the P-domain (green region) of the CP monomer interacts with the P-domain/E-loop (green/yellow region) of a CP subunit of the hexamer. However, the E-loops/Telokin-domain (yellow/purple region) of the CP monomer and the other CP subunit of the hexamer are further away in structure (g) due to the sterical hindrance from SP2.

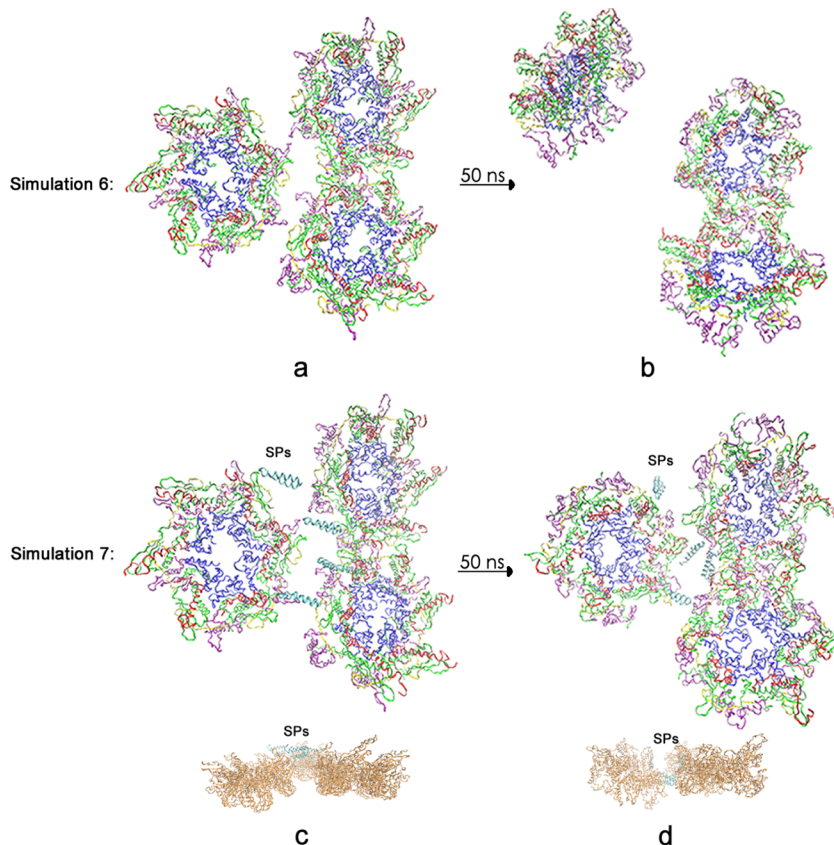


**Figure 4.** Simulations 6–7: SP C-terminal mediated aggregation between disconnected hexamer and dihexamer for 50 ns. The configurations in simulation 7 are shown in both top and side views to present the curvature change. (a) SP free initial configuration in simulation 6. (b) Configuration after 50 ns of simulation 6. (c) Initial configuration in simulation 7, with four SP C-terminal monomers located on the interface of hexamers. (d) Configuration after 50 ns of simulation 7; the curvature of the overall structure is gradually mediated but the hexamers are not attached.

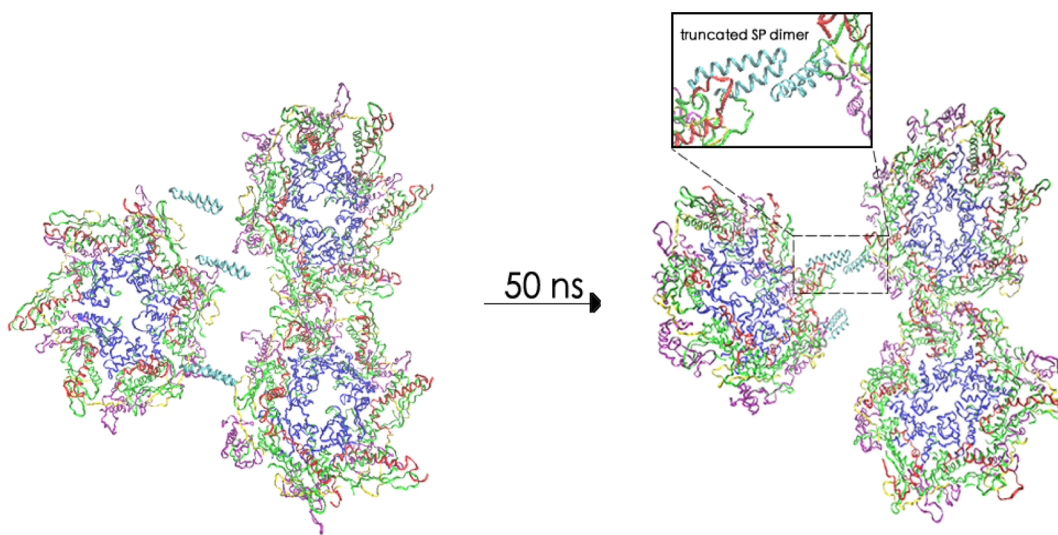


**Figure 5.** Trial simulation revealing SP C-terminal dimer being stabilized by loop interaction.

results agree with the previous experimental results, suggesting that the geometric constraint provided by interactions between SP and CP is important for the efficiency and fidelity of intracapsomer dimerization of CP monomer. Also, a capsomer may emerge with step-by-step monomer addition similar to the CP dimerization mechanism described here.

In contrast to the well-understood CP-binding domain in a SP structure, the SP-binding sites in CP structure remain unclear in

P22 self-assembly. The details of the configuration after 20 ns of simulation 2 reveal SP C-terminal binding sites in CP (Table 1, Figure S1-a in Supporting Information), which demonstrate that dimerization involves the interactions between SP C-terminal and multiple structural domains of CP.

## 2.2. SP C-Terminal Mediated Complexing of CP

**Monomer and Capsomer.** It was argued that approximately 140–300 SPs per capsid are required to obtain  $T = 7$  structure in

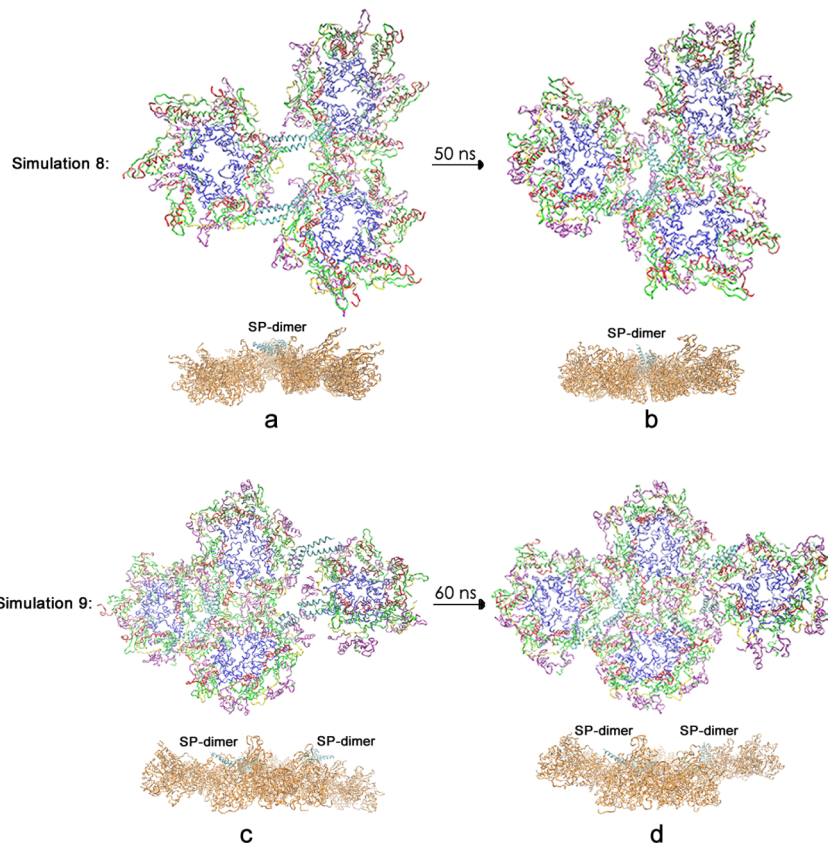


**Figure 6.** Simulations 8–9: SP C-terminal dimer mediated aggregation between capsomers. All the configurations are shown in both top and side views to present the structural change. (a) Initial configuration in simulation 8, with two SP C-terminal dimers located at the interface of hexamers. (b) Configuration after 50 ns of simulation 8; both aggregation and formation of correct curvature of hexamers occur. (c) Initial configuration in simulation 9 obtained from the configuration after 50 ns of simulation 8, with two more SP C-terminal dimers located at the interface of hexamers and pentamer. (d) Configuration after 60 ns of simulation 9; both attachment and formation of correct curvature of hexamers and pentamer occur.

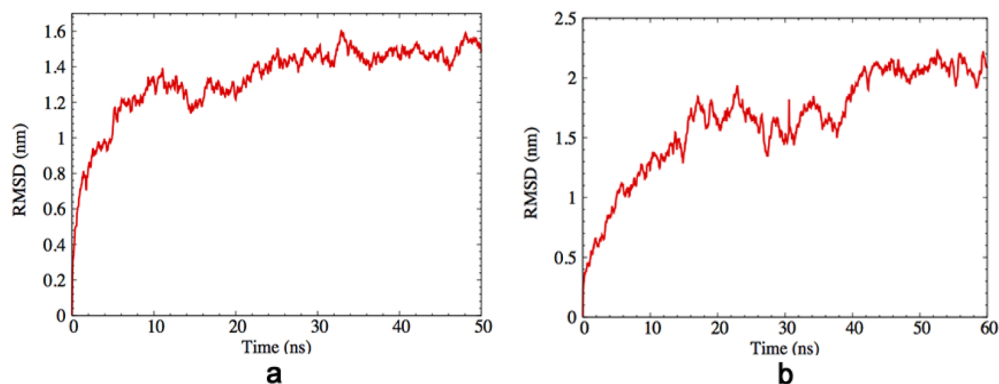


**Figure 7.** RMSD analysis shows that the curvatures formed in simulation 8 (a) and 9 (b) are stabilized.

P22 self-assembly.<sup>14</sup> With a concentration lower than this range *in vitro*, the dominating species would be the intermediate structures of capsid. Abundance of SP-binding sites in a CP capsomer suggests that the SP/CP concentration ratio can affect the occupancy of these binding sites, and consequently alter the efficiency of the overall P22 self-assembly. To examine this idea, 30 ns simulations were performed with different numbers (0, 1, and 2) of SP C-terminals but the same initial configuration of a CP monomer and a hexamer (simulations 3–5). In the SP C-terminal free simulation 3 (Figure 3a), complexing did not occur between CP and hexamer (Figure 3b). With one SP C-terminal initially near the N-arm/P-domain of CP monomer in simulation

4 (Figure 3c), these two structural domains of CP monomer approach hexamer (Figure 3d). With SP C-terminals placed near both N-arm/P-domain and E-loop in simulation 5 (Figure 3e), CP monomer approaches the hexamer at 10 ns (Figure 3f); and CP monomer and hexamer are attached at 30 ns (Figure 3g). The configuration after 30 ns of simulation 5 is similar to that of a hexamer plus a neighboring CP subunit in P22 capsid (Figure 3i). Though the above simulations were carried out to show the complexing of a CP monomer and a hexamer, the same pathway is expected for the complexing of a CP monomer and a pentamer based on the high similarity between the structures of a hexamer plus a neighboring CP subunit (Figure 3i) and those of a

pentamer plus a neighboring CP subunit (Figure 3h) in P22 capsid.

The details of the SP C-terminal binding sites in CP monomer/hexamer are collected from simulations 4 and 5 (Table 2, Figure S1 b–f in Supporting Information). The participation of multiple domains of CP structure present in simulations 2, 4, and 5 is likely to be important for SP/CP recognition efficiency, as well as for overcoming the disorganizing factors such as mutations or cleavage of part of P22 capsid subunits, and consequently enhances the fidelity of the process in different environments.

**2.3. SP C-Terminal-Mediated Aggregation of CP Capsomers.** As P22 self-assembly proceeds, larger intermediate structures with multiple capsomers emerge. In addition to controlling the aggregation of capsomers, one may also wonder how a curvature corresponding to a  $T = 7$  capsid can be maintained for these intermediate structures. To capture the details of this process, an initial configuration is considered involving a disconnected hexamer and a dihexamer. 50 ns simulations are performed to explore the pathway of self-assembly with and without SP C-terminals (Figure 4a,c). Without SP C-terminals, the disconnected hexamer randomly walks away from the dihexamer (simulation 6, Figure 4b). With four SP C-terminal monomers bridging the hexamers, the larger structure is assembled, although the hexamers are not attached completely (simulation 7, Figure 4d).

The SP C-terminal devoid of R74C/L177I residues was believed to activate CP assembly as monomer.<sup>20</sup> However, a SP C-terminal dimer structure with a conformation distinct from that of covalently bonded SP dimer is discovered through simulation, which is stabilized by loop interaction (Figure 5). The SP C-terminal dimer is demonstrated to facilitate capsomer aggregation, and eventually induce a structure with curvature similar to that of P22 capsid (simulations 8 and 9, Figure 6). RMSD analysis show that the curvatures formed in both simulations 8 and 9 are stabilized (Figure 7). Detailed inspection of the binding sites between SP C-terminal dimers and the intermediate structures reveals how SP C-terminal dimers mediate the curvature formation of them (Figure S2 in Supporting Information). The E-loops (yellow) and Telokin-domains (purple) from different capsomers gradually approach each other, and interactions between SP C-terminal dimers and N-arms/P-domains (red/green) from them simultaneously change the curvature of the overall structures. These observations are consistent with the hypotheses explaining SP's role in capsid size regulation.<sup>19</sup>

The influence of SP C-terminal dimers is as follows. First, the extended structure of SP C-terminal dimer can bridge the capsomers more efficiently and is less likely to be dislocated in the multiple binding sites of a capsomer. Second, the SP C-terminal dimer provides proper interaction as well as sterical hindrance to maintain the correct curvature of the intermediate structures. Nevertheless, it was observed that a high concentration of SP can limit the rate of P22 self-assembly.<sup>18</sup> A possible explanation is that excess SP polymers located on the interface of the capsomers would inhibit the attachment of capsomers as well as capsid curvature formation.

Distinct from the oriented SP dimer with covalent bond, the SP C-terminal dimer linked through electrostatic interaction discovered in the present study provides more accessible conformations. The coexistence of multiple SP C-terminal dimer conformations, like the participation of multiple structural domains of CP, is probably important for efficient dimerization

and overcoming the disorganizing factors during self-assembly. The observed lower fidelity<sup>20</sup> of capsid formation when R74C/L177I residues are missing can be explained in terms of the fewer numbers of SP dimer conformations with the truncation.

### 3. CONCLUSION

Early stage P22 self-assembly mediated by SP C-terminal is studied via atom-resolved simulation. The diverse binding patterns (SP C-terminal monomer/CP monomer, SP C-terminal monomer/CP capsomer, and SP C-terminal dimer/CP capsomer), SP concentration effect and a SP C-terminal dimer with new conformation are presented computationally. The phenomena identified appear to be critical for the efficiency, fidelity, and capsid curvature of P22 self-assembly. Results presented here suggest a similar approach could be used to study self-assembly of other viral capsids, and more accurate coarse-grained models can be built on the present finding.

Further understanding of P22 self-assembly obtained in this study can be important for applications such as antiviral drug discovery and capsid-based nanoplatform design. One of the possible strategies to develop antiviral drugs is to interrupt viral capsid self-assembly. In addition, the involvement of multiple structural domains of CP, and different conformations of SP C-terminal dimer, is suggested to be important for overcoming the disorganizing factors in self-assembly, which also imply that P22 capsid is a reasonable starting point for nanoplatform design. With appropriate residue modification or mutation, self-assembly can still occur and induce a capsid with desired structure and function.

### ■ ASSOCIATED CONTENT

#### Supporting Information

Preparations to MD simulations, structure modeling, structure visualization, and supplementary simulation results included. This material is available free of charge via the Internet at <http://pubs.acs.org>.

### ■ AUTHOR INFORMATION

#### Corresponding Author

\*E-mail: ortoleva@indiana.edu.

#### Notes

The authors declare no competing financial interest.

### ■ ACKNOWLEDGMENTS

This project was supported in part by the National Science Foundation (Collaborative Research in Chemistry Program), NSF INSPIRE program, National Institutes of Health (NIBIB), Indiana University College of Arts and Sciences, and the Indiana University information technology services (UIT) high performance computing resources.

### ■ REFERENCES

- (1) Cadena-Nava, R. D.; Comas-Garcia, M.; Garmann, R. F.; Rao, A.; Knobler, C. M.; Gelbart, W. M. Self-Assembly of Viral Capsid Protein and RNA Molecules of Different Sizes: Requirement for a Specific High Protein/RNA Mass Ratio. *J. Virol.* 2012, 86, 3318–3326.
- (2) Bruinsma, R. F.; Gelbart, W. M.; Reguera, D.; Rudnick, J.; Zandi, R. Viral Self-Assembly As a Thermodynamic Process. *Phys. Rev. Lett.* 2003, 90, 248101.
- (3) Prevelige Jr., P. E. Inhabiting Virus-Capsid Assembly by Altering Polymerisation Pathways. *Trends Biotechnol.* 1998, 16, 61–65.
- (4) Patterson, D. P.; Schwarz, B.; El-Boubbou, K.; van der Oost, J.; Prevelige, P. E.; Douglas, T. Virus-Like Particle Nanoreactors:

- Programmed Encapsulation of the Thermostable CelB Glycosidase inside the P22 Capsid. *Soft Matter* **2012**, *8*, 10158–10166.
- (5) Patterson, D. P.; Schwarz, B.; Waters, R. S.; Gedeon, T.; Douglas, T. Encapsulation of an Enzyme Cascade within the Bacteriophage P22 Virus-Like Particle. *ACS Chem. Biol.* **2013**, *9*, 359–365.
- (6) Rome, L. H.; Kickhoefer, V. A. Development of the Vault Particle As a Platform Technology. *ACS Nano* **2012**, *7*, 889–902.
- (7) Servid, A.; Jordan, P.; O’Neil, A.; Prevelige, P.; Douglas, T. Location of the Bacteriophage P22 Coat Protein C-Terminus Provides Opportunities for the Design of Capsid-Based Materials. *Biomacromolecules* **2013**, *14*, 2989–2995.
- (8) Caspar, D.; Dulbecco, R.; Klug, A.; Lwoff, A.; Stoker, M.; Tournier, P.; Wildy, P. Proposals. *Cold Spring Harbor Symp. Quant. Biol.* **1962**, *27*, 49–50.
- (9) King, J.; Casjens, S. Catalytic Head Assembling Protein in Virus Morphogenesis. *Nature* **1974**, *251*, 112–119.
- (10) Casjens, S.; King, J. P22 Morphogenesis I: Catalytic Scaffolding Protein in Capsid Assembly. *J. Supramol. Struct.* **1974**, *2*, 202–224.
- (11) Parker, M. H.; Prevelige Jr, P. E. Electrostatic Interactions Drive Scaffolding/Coat Protein Binding and Procapсид Maturation in Bacteriophage P22. *Virology* **1998**, *250*, 337–349.
- (12) Sun, Y.; Parker, M. H.; Weigle, P.; Casjens, S.; Prevelige Jr, P. E.; Krishna, N. R. Structure of the Coat Protein-Binding Domain of the Scaffolding Protein from a Double-Stranded DNA Virus. *J. Mol. Biol.* **2000**, *297*, 1195–1202.
- (13) Casjens, S.; Adams, M. B. Posttranscriptional Modulation of Bacteriophage P22 Scaffolding Protein Gene Expression. *J. Virol.* **1985**, *53*, 185–191.
- (14) Prevelige Jr, P. E.; Thomas, D.; King, J. Scaffolding Protein Regulates the Polymerization of P22 Coat Subunits into Icosahedral Shells in Vitro. *J. Mol. Biol.* **1988**, *202*, 743–757.
- (15) Prevelige Jr, P. E.; Thomas, D.; King, J. Nucleation and Growth Phases in the Polymerization of Coat and Scaffolding Subunits into Icosahedral Procapсид Shells. *Biophys. J.* **1993**, *64*, 824–835.
- (16) Earnshaw, W.; Casjens, S.; Harrison, S. C. Assembly of the Head of Bacteriophage P22: X-Ray Diffraction from Heads, Proheads and Related Structures. *J. Mol. Biol.* **1976**, *104*, 387–410.
- (17) Greene, B.; King, J. Binding of Scaffolding Subunits within the P22 Procapвид Lattice. *Virology* **1994**, *205*, 188–197.
- (18) Caspar, D.; Klug, A. Physical Principles in the Construction of Regular Viruses. *Cold Spring Harbor Symp. Quant. Biol.* **1962**, *27*, 1–24.
- (19) Johnson, J. E.; Speir, J. A. Quasi-Equivalent Viruses: A Paradigm for Protein Assemblies. *J. Mol. Biol.* **1997**, *269*, 665–675.
- (20) Tuma, R.; Tsuruta, H.; French, K. H.; Prevelige, P. E. Detection of Intermediates and Kinetic Control during Assembly of Bacteriophage P22 Procapвид. *J. Mol. Biol.* **2008**, *381*, 1395–1406.
- (21) Parker, M. H.; Stafford III, W. F.; Prevelige Jr, P. E. Bacteriophage P22 Scaffolding Protein Forms Oligomers in Solution. *J. Mol. Biol.* **1997**, *268*, 655–665.
- (22) Parker, M. H.; Casjens, S.; Prevelige Jr, P. E. Functional Domains of Bacteriophage P22 Scaffolding Protein. *J. Mol. Biol.* **1998**, *281*, 69–79.
- (23) Weigle, P. R.; Sampson, L.; Winn-Stapley, D.; Casjens, S. R. Molecular Genetics of Bacteriophage P22 Scaffolding Protein’s Functional Domains. *J. Mol. Biol.* **2005**, *348*, 831–844.
- (24) Cortines, J. R.; Weigle, P. R.; Gilcrease, E. B.; Casjens, S. R.; Teschke, C. M. Decoding Bacteriophage P22 Assembly: Identification of Two Charged Residues in Scaffolding Protein Responsible for Coat Protein Interaction. *Virology* **2011**, *421*, 1–11.
- (25) Parent, K. N.; Khayat, R.; Tu, L. H.; Suhannovsky, M. M.; Cortines, J. R.; Teschke, C. M.; Johnson, J. E.; Baker, T. S. P22 Coat Protein Structures Reveal a Novel Mechanism for Capsid Maturation: Stability without Auxiliary Proteins or Chemical Crosslinks. *Structure* **2010**, *18*, 390–401.
- (26) Thuman-Commike, P. A.; Greene, B.; Jakana, J.; McGough, A.; Prevelige, P. E.; Chiu, W. Identification of Additional Coat-Scaffolding Interactions in a Bacteriophage P22 Mutant Defective in Maturation. *J. Virol.* **2000**, *74*, 3871–3873.
- (27) Chen, D.-H.; Baker, M. L.; Hryc, C. F.; DiMaio, F.; Jakana, J.; Wu, W.; Dougherty, M.; Haase-Pettingell, C.; Schmid, M. F.; Jiang, W. Structural Basis for Scaffolding-Mediated Assembly and Maturation of a dsDNA Virus. *Proc. Natl. Acad. Sci. U. S. A.* **2011**, *108*, 1355–1360.
- (28) Cortines, J. R.; Motwani, T.; Vyas, A. A.; Teschke, C. M. Highly Specific Salt Bridges Govern Bacteriophage P22 Icosahedral Capsid Assembly: Identification of the Site in Coat Protein Responsible for Interaction with Scaffolding Protein. *J. Virol.* **2014**, *88*, 5287–5297.
- (29) Rapaport, D.; Johnson, J.; Skolnick, J. Supramolecular Self-Assembly: Molecular Dynamics Modeling of Polyhedral Shell Formation. *Comput. Phys. Commun.* **1999**, *121*, 231–235.
- (30) Rapaport, D. Self-Assembly of Polyhedral Shells: A Molecular Dynamics Study. *Phys. Rev. E: Stat., Nonlinear, Soft Matter Phys.* **2004**, *70*, 051905.
- (31) Ross, P. D.; Conway, J. F.; Cheng, N.; Dierkes, L.; Firek, B. A.; Hendrix, R. W.; Steven, A. C.; Duda, R. L. A Free Energy Cascade with Locks Drives Assembly and Maturation of Bacteriophage HK97 Capsid. *J. Mol. Biol.* **2006**, *364*, 512–525.
- (32) Arkhipov, A.; Freddolino, P. L.; Schulten, K. Stability and Dynamics of Virus Capsids Described by Coarse-Grained Modeling. *Structure* **2006**, *14*, 1767–1777.
- (33) Hagan, M. F.; Chandler, D. Dynamic Pathways for Viral Capsid Assembly. *Biophys. J.* **2006**, *91*, 42–54.
- (34) Nguyen, H. D.; Reddy, V. S.; Brooks, C. L. Deciphering the Kinetic Mechanism of Spontaneous Self-Assembly of Icosahedral Capsids. *Nano Lett.* **2007**, *7*, 338–344.
- (35) McCammon, J. A.; Gelin, B. R.; Karplus, M. Dynamics of Folded Proteins. *Nature* **1977**, *267*, 585–590.
- (36) Karplus, M.; McCammon, J. A. Molecular Dynamics Simulations of Biomolecules. *Nat. Struct. Mol. Biol.* **2002**, *9*, 646–652.